

# Symmetry-based atomic scale description of lattice dynamics and its applications for phonon mode analysis

Jichan Moon,<sup>1</sup> Tsezar F. Seman,<sup>2</sup> and K. H. Ahn<sup>2,\*</sup>

<sup>1</sup>*Department of Physics, Konkuk University, Seoul, 143-701, South Korea*

<sup>2</sup>*Department of Physics, New Jersey Institute of Technology, Newark, New Jersey 07102, USA*

We present classical and quantum mechanical multiscale descriptions of lattice dynamics, from the atomic to the continuum scale, using atomic scale symmetry modes and their constraint equations. This approach is demonstrated for a one-dimensional chain and a two-dimensional square lattice with a monatomic basis. For the classical description, we find that rigid modes, in addition to the distortional modes found before, are necessary to describe the kinetic energy, and obtain constraint equations among these modes. Lagrangian equations, modified with the Lagrange multiplier terms, are solved for phonon dispersion relations without using displacement variables explicitly. The long wavelength limit of the kinetic energy terms expressed in terms of atomic scale modes is shown to be consistent with the continuum theory, and the leading order corrections are obtained. We also analyze the phonon in terms of symmetry modes, and find how the contribution of different symmetry modes varies depending on the phonon branch and wavevector. For the quantum mechanical description, we find conjugate momenta for the atomic scale symmetry modes. In direct space, graphical rules for their commutation relations are obtained. Commutation relations in the reciprocal space are also calculated. We emphasize that the approach based on atomic scale symmetry modes could be useful for the description of multiscale lattice dynamics, materials with electron-phonon coupling, and the dynamics of structural phase transition, which can be probed by time-resolved x-ray diffraction.

PACS numbers: 61.50.Ah, 63.20.D-, 63.22.-m, 62.20.-x

## I. INTRODUCTION

The dynamics at nanometer length scale has been a focus of recent attention.<sup>1</sup> In particular, materials with competing ground states, such as high temperature superconducting cuprates and colossal magnetoresistive manganites,<sup>2,3,4</sup> often show dynamic nanometer scale features, for example, stripes in cuprates<sup>5,6</sup> and anisotropic correlations in manganites.<sup>7,8</sup> Furthermore, recent advances in time-resolved x-ray technique have allowed experimenters to directly probe lattice dynamics in atomic scale.<sup>9</sup> It is believed that understanding these nanoscale features and their dynamics is essential to explain macroscopic properties of these materials.

For the description of mesoscopic scale domain structures and their dynamics, phenomenological Ginzburg-Landau formalism has been very successful.<sup>10,11</sup> One of the keys for such a success is the use of symmetry in the definition of variables, which makes the selection of free energy terms self-evident. Motivated by the success of the Ginzburg-Landau approach for the continuum, symmetry-based atomic scale description of lattice distortions has been recently proposed, and demonstrated for a two-dimensional square lattice.<sup>12</sup> In this approach, atomic scale symmetry modes are defined on a plaquette of atoms, and are used to express potential energy terms associated with lattice distortions. This method has been used to understand atomic scale structure of twin boundaries,<sup>12</sup> antiphase boundaries and their electronic textures,<sup>13</sup> strain-induced metal-insulator phase coexistence in manganites,<sup>8</sup> superconducting order parameter textures around structural defects,<sup>14</sup> and the coupling be-

tween electronic nematic order parameter and structural domains in metamagnets near a quantum critical point.<sup>15</sup> Thus far, this approach has been used for static lattices, or the relaxation of lattice distortions introduced through the Euler method,<sup>10</sup> which does not require kinetic energy terms. In the current paper, we present our study on how the approach based on atomic scale symmetry modes can be extended to describe lattice dynamics, within the scope of both classical and quantum mechanical formalism.<sup>16</sup> In Section II, we discuss how to express kinetic energy term in symmetry modes, present our study within the formalism of classical mechanics, compare our result with the continuum results,<sup>11</sup> and analyze the phonon spectrum in terms of symmetry modes. We formulate quantum mechanics in terms of atomic scale symmetry modes in Section III, with a summary given in Section IV.

## II. CLASSICAL FORMALISM

### A. One-dimensional lattice with a monatomic basis

Using a one-dimensional lattice with a monatomic basis shown in Fig. 1, we demonstrate mode-based description of lattice dynamics. The displacements of atoms are

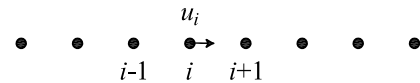


FIG. 1: One-dimensional lattice with a monatomic basis.

represented by  $u_i$ , where  $i$  being an index for the site. To be specific, we assume that the interaction between the nearest neighbor atoms are described by a spring with a spring constant  $K$  while other potential energy terms are negligible, as represented by the following Lagrangian,

$$L_{\text{chain}} = \sum_i \frac{1}{2} M \dot{u}_i^2 - \frac{1}{2} K (u_{i+1} - u_i)^2, \quad (1)$$

where  $M$  is the mass of the atom. We take a two-atom unit as a motif for this lattice, and define the symmetry modes,  $e(i)$  and  $t(i)$ ,

$$e(i) \equiv \frac{1}{\sqrt{2}}(u_{i+1} - u_i), \quad (2)$$

$$t(i) \equiv \frac{1}{\sqrt{2}}(u_{i+1} + u_i), \quad (3)$$

where a normalization factor is chosen according to the number of displacement variables in the definition. These modes are also shown in Fig. 2.

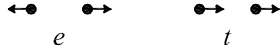


FIG. 2: Symmetry modes for the one-dimensional chain in Fig. 1.

The two variables,  $e$  and  $t$ , correspond to the distortion and rigid translation of the motif, respectively. Since the two modes are defined from one physically independent displacement variable at each site  $i$ , these modes are related through one constraint equation shown below in the reciprocal space and direct space, respectively.

$$f(k) \equiv (e^{ik} + 1)e(k) - (e^{ik} - 1)t(k) = 0, \quad (4)$$

$$e(i+1) + e(i) - t(i+1) + t(i) = 0. \quad (5)$$

In terms of these modes, the Lagrangian in Eq. (1) is expressed in the following way

$$L_{\text{chain}} = \sum_i \frac{1}{2} \left( \frac{M}{2} \right) [\dot{e}(i)^2 + \dot{t}(i)^2] - \frac{1}{2} (2K) e(i)^2. \quad (6)$$

The result shows that introduction of atomic scale rigid modes, such as  $t$ , which are not considered in Ref. 12, allows kinetic energy term being expressed in a quadratic form. To obtain equations of motion, we modify  $L_{\text{chain}}$  with a Lagrange multiplier  $\lambda(k)$ , as shown below.

$$\begin{aligned} \tilde{L}_{\text{chain}} = & \sum_k \frac{1}{2} \left( \frac{M}{2} \right) [\dot{e}(k)\dot{e}(-k) + \dot{t}(k)\dot{t}(-k)] \\ & - \frac{1}{2} (2K) e(k)e(-k) + \lambda(k)f(-k). \end{aligned} \quad (7)$$

The Lagrangian formalism of dynamics leads to the two equations of motion,

$$\frac{M}{2} \ddot{e}(k) + 2K e(k) - \lambda(k)(e^{-ik} + 1) = 0, \quad (8)$$

$$\frac{M}{2} \ddot{t}(k) + \lambda(k)(e^{-ik} - 1) = 0, \quad (9)$$

and a well-known dispersion relation for the one-dimensional chain,<sup>17</sup>

$$\omega = \sqrt{\frac{K}{M}} (1 - \cos k). \quad (10)$$

This result shows that the lattice dynamics can be studied within the framework of atomic scale symmetry modes and their constraint equations, without using the displacement variables explicitly.

Anharmonicity of one-dimensional chains is important to understand non-linear excitations, such as solitons, kink-solitons, intrinsically localized modes, and breathers.<sup>18,19</sup> Atomic scale modes,  $e$  and  $t$ , found here can be used to incorporate such anharmonicity into the Hamiltonian, which, along with their constraint equations, would provide a formalism to study the dynamics of non-linear excitations in one-dimensional chains. In the next subsection, we demonstrate how the mode-based approach is applied to lattice dynamics for a two-dimensional square lattice with a monatomic basis.

## B. Two-dimensional square lattice with a monatomic basis

Symmetry-based atomic scale description of lattice distortions for a two-dimensional square lattice with a monatomic basis, shown in Fig. 3, has been studied in Ref. 12, where dilatational  $e_1$ , shear  $e_2$ , and deviatoric  $e_3$  modes, and short wavelength modes,  $s_x$  and  $s_y$ , are defined, as shown in Fig. 4. In terms of displacement variables  $u_i^x$  and  $u_i^y$ , and  $i_x$  and  $i_y$  representing site indices, these distortional symmetry modes are expressed

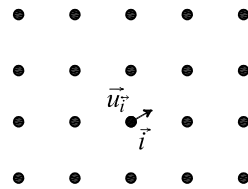


FIG. 3: Two-dimensional square lattice with a monatomic basis.

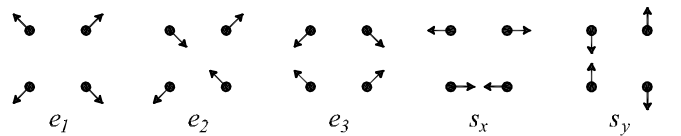


FIG. 4: Distortional symmetry modes of the motif for the two-dimensional square lattice with a monatomic basis in Fig. 3.

as follows.

$$e_1(\vec{i}) = \frac{1}{2\sqrt{2}} \left( -u_i^x - u_i^y + u_{i+10}^x - u_{i+10}^y - u_{i+01}^x + u_{i+01}^y + u_{i+11}^x + u_{i+11}^y \right), \quad (11)$$

$$e_2(\vec{i}) = \frac{1}{2\sqrt{2}} \left( -u_i^x - u_i^y - u_{i+10}^x + u_{i+10}^y + u_{i+01}^x - u_{i+01}^y + u_{i+11}^x + u_{i+11}^y \right), \quad (12)$$

$$e_3(\vec{i}) = \frac{1}{2\sqrt{2}} \left( -u_i^x + u_i^y + u_{i+10}^x + u_{i+10}^y - u_{i+01}^x - u_{i+01}^y + u_{i+11}^x - u_{i+11}^y \right), \quad (13)$$

$$s_x(\vec{i}) = \frac{1}{2} \left( u_i^x - u_{i+10}^x - u_{i+01}^x + u_{i+11}^x \right), \quad (14)$$

$$s_y(\vec{i}) = \frac{1}{2} \left( u_i^y - u_{i+10}^y - u_{i+01}^y + u_{i+11}^y \right). \quad (15)$$

Instead of  $s_x$  and  $s_y$  modes, the following  $s_+$  and  $s_-$  modes can be also used.

$$s_+(\vec{i}) = \frac{1}{\sqrt{2}} [s_x(\vec{i}) + s_y(\vec{i})], \quad (16)$$

$$s_-(\vec{i}) = \frac{1}{\sqrt{2}} [s_x(\vec{i}) - s_y(\vec{i})]. \quad (17)$$

These five modes have been used to express various harmonic and anharmonic potential energy terms,<sup>8,12,13</sup> but are not sufficient to represent kinetic energy terms in a simple quadratic form. For example, an expression has been converted back to the displacement variables to obtain the phonon spectrum shown in Fig. 2 in Ref. 12.

In current work, we show that additional modes associated with the rigid motion of the motif, similar to the mode  $t$  in the one-dimensional chain, allow a formalism entirely based on symmetry modes without resorting to displacement variables. Three rigid modes for the two-dimensional square lattice are shown in Fig. 5 and are defined as follows.

$$t_x(\vec{i}) = \frac{1}{2} \left( u_i^x + u_{i+10}^x + u_{i+01}^x + u_{i+11}^x \right), \quad (18)$$

$$t_y(\vec{i}) = \frac{1}{2} \left( u_i^y + u_{i+10}^y + u_{i+01}^y + u_{i+11}^y \right), \quad (19)$$

$$r(\vec{i}) = \frac{1}{2\sqrt{2}} \left( u_i^x - u_i^y + u_{i+10}^x + u_{i+10}^y - u_{i+01}^x - u_{i+01}^y - u_{i+11}^x + u_{i+11}^y \right). \quad (20)$$

The first two modes,  $t_x$  and  $t_y$ , correspond to rigid translations of the motif along  $x$  and  $y$  direction, and the mode  $r$  represents a rigid rotation of the motif. Following  $t_+$  and  $t_-$  modes can be also used as alternatives to  $t_x$  and  $t_y$ .

$$t_+(\vec{i}) = \frac{1}{\sqrt{2}} [t_x(\vec{i}) + t_y(\vec{i})], \quad (21)$$

$$t_-(\vec{i}) = \frac{1}{\sqrt{2}} [t_x(\vec{i}) - t_y(\vec{i})]. \quad (22)$$

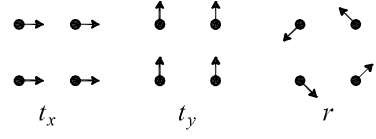


FIG. 5: Rigid symmetry modes of the motif for the two-dimensional square lattice with a monatomic basis in Fig. 3.

Straight-forward expansion shows that the kinetic energy of the lattice is expressed in terms of the eight symmetry modes in the following quadratic form, with  $M$  being the mass of the atom.

$$T_{\text{sq}} = \sum_{\vec{i}} \frac{1}{2} M [(\dot{u}_i^x)^2 + (\dot{u}_i^y)^2] \quad (23)$$

$$= \sum_{\vec{i}} \frac{1}{2} \left( \frac{M}{4} \right) [\dot{e}_1(\vec{i})^2 + \dot{e}_2(\vec{i})^2 + \dot{e}_3(\vec{i})^2 + \dot{s}_x(\vec{i})^2 + \dot{s}_y(\vec{i})^2 + \dot{t}_x(\vec{i})^2 + \dot{t}_y(\vec{i})^2 + \dot{r}(\vec{i})^2]. \quad (24)$$

As discussed in Ref. 12, constraint equations are found from the relations between symmetry modes and displacement variables in the reciprocal space. We first represent  $(u_k^x, u_k^y)$  in terms of  $(s_x(\vec{k}), s_y(\vec{k}))$  by inverting the linear relations between them, and replace in the expressions with other modes, which lead to six constraint equations.<sup>20</sup>

$$\sin \frac{k_x}{2} \cos \frac{k_y}{2} s_x(\vec{k}) + \cos \frac{k_x}{2} \sin \frac{k_y}{2} s_y(\vec{k}) - \sqrt{2}i \sin \frac{k_x}{2} \sin \frac{k_y}{2} e_1(\vec{k}) = 0, \quad (25)$$

$$\cos \frac{k_x}{2} \sin \frac{k_y}{2} s_x(\vec{k}) + \sin \frac{k_x}{2} \cos \frac{k_y}{2} s_y(\vec{k}) - \sqrt{2}i \sin \frac{k_x}{2} \sin \frac{k_y}{2} e_2(\vec{k}) = 0, \quad (26)$$

$$\sin \frac{k_x}{2} \cos \frac{k_y}{2} s_x(\vec{k}) - \cos \frac{k_x}{2} \sin \frac{k_y}{2} s_y(\vec{k}) - \sqrt{2}i \sin \frac{k_x}{2} \sin \frac{k_y}{2} e_3(\vec{k}) = 0, \quad (27)$$

$$\cos \frac{k_x}{2} \sin \frac{k_y}{2} s_x(\vec{k}) - \sin \frac{k_x}{2} \cos \frac{k_y}{2} s_y(\vec{k}) + \sqrt{2}i \sin \frac{k_x}{2} \sin \frac{k_y}{2} r(\vec{k}) = 0, \quad (28)$$

$$\cos \frac{k_x}{2} \cos \frac{k_y}{2} s_x(\vec{k}) + \sin \frac{k_x}{2} \sin \frac{k_y}{2} t_x(\vec{k}) = 0, \quad (29)$$

$$\cos \frac{k_x}{2} \cos \frac{k_y}{2} s_y(\vec{k}) + \sin \frac{k_x}{2} \sin \frac{k_y}{2} t_y(\vec{k}) = 0. \quad (30)$$

Modified Lagrangian for the square lattice is now

$$\tilde{L}_{\text{sq}} = T_{\text{sq}} - V + \sum_{n=1}^6 \sum_{\vec{k}} \lambda_n(\vec{k}) f_n(-\vec{k}), \quad (31)$$

where  $V$  is the potential energy,  $\lambda_n(\vec{k})$  are Lagrange multipliers, and  $f_n(\vec{k}) = 0$  are the six constraint equations, Eqs. (25) - (30). By solving the Lagrangian equations, we find dynamic properties of the lattice in terms of the symmetry modes. As with the Ginzburg-Landau approach being useful for the description of mesoscale dynamics, we expect that the approach based on atomic

scale symmetry modes would be useful for the description of atomic scale dynamics, particularly, when anharmonicity plays an essential role. In the next two subsections, we present two applications of the formalism developed in this subsection.

### C. Comparison with continuum description of lattice dynamics

We compare the atomic scale theory developed in the previous subsection with an existing continuum theory of lattice dynamics. Either by using the definitions, Eqs. (11) and (13), or by using the constraint equations, we express the kinetic energy for the square lattice, Eqs. (23) and (24), in terms of  $e_1$  and  $e_3$ ,

$$T_{\text{sq}} = \sum_{\vec{k}} \sum_{s=1,3} \sum_{s'=1,3} \frac{1}{2} M \gamma_{ss'}(\vec{k}) \dot{e}_s(\vec{k}) \dot{e}_{s'}(-\vec{k}), \quad (32)$$

where

$$\gamma_{11}(\vec{k}) = \gamma_{33}(\vec{k}) = \frac{1 - \cos k_x \cos k_y}{\sin^2 k_x \sin^2 k_y}, \quad (33)$$

$$\gamma_{13}(\vec{k}) = \gamma_{31}(\vec{k}) = \frac{\cos k_x - \cos k_y}{\sin^2 k_x \sin^2 k_y}. \quad (34)$$

To compare with a continuum theory, we take the long wavelength limit, and obtain the following leading order term for  $\gamma_{ss'}$ ,

$$\gamma_{ss'}^{(0)}(\vec{k}) = \begin{pmatrix} \frac{k_x^2 + k_y^2}{2k_x^2 k_y^2} & \frac{k_y^2 - k_x^2}{2k_x^2 k_y^2} \\ \frac{k_y^2 - k_x^2}{2k_x^2 k_y^2} & \frac{k_x^2 + k_y^2}{2k_x^2 k_y^2} \end{pmatrix}. \quad (35)$$

This term is identical to Eq. (3.12a) in Ref. 11 ( $e_3$  here corresponds to  $e_2$  in Ref. 11), which Lookman *et al.* have used as continuum kinetic energy to study underdamped dynamics of strains in proper ferroelastic materials. The next order term to the above continuum limit is as follows.

$$\gamma_{ss'}^{(1)}(\vec{k}) = \begin{pmatrix} \frac{1}{12} + \frac{k_x^4 + k_y^4}{8k_x^2 k_y^2} & \frac{k_y^4 - k_x^4}{8k_x^2 k_y^2} \\ \frac{k_y^4 - k_x^4}{8k_x^2 k_y^2} & \frac{1}{12} + \frac{k_x^4 + k_y^4}{8k_x^2 k_y^2} \end{pmatrix}. \quad (36)$$

This term, or better Eqs. (33) and (34), can be used to study the dynamics of proper ferroelastic materials on the atomic scale. The following long wavelength limit of the atomic scale modes shows directly what they correspond

to in the continuum theory.

$$e_1(\vec{i}) = \frac{1}{\sqrt{2}} [\nabla_x u_i^x + \nabla_y u_i^y], \quad (37)$$

$$e_2(\vec{i}) = \frac{1}{\sqrt{2}} [\nabla_x u_i^y + \nabla_y u_i^x], \quad (38)$$

$$e_3(\vec{i}) = \frac{1}{\sqrt{2}} [\nabla_x u_i^x - \nabla_y u_i^y], \quad (39)$$

$$r(\vec{i}) = \frac{1}{\sqrt{2}} [\nabla_x u_i^y - \nabla_y u_i^x], \quad (40)$$

$$s_x(\vec{i}) = \frac{1}{2} \nabla_x \nabla_y u_i^x, \quad (41)$$

$$s_y(\vec{i}) = \frac{1}{2} \nabla_x \nabla_y u_i^y, \quad (42)$$

$$t_x(\vec{i}) = 2u_i^x, \quad (43)$$

$$t_y(\vec{i}) = 2u_i^y. \quad (44)$$

In  $k \rightarrow 0$  limit, the correspondence of these modes to the displacements  $u$  are

$$\begin{aligned} t_x, t_y &\sim u, \\ e_1, e_2, e_3, r &\sim ku, \\ s_x, s_y &\sim k^2 u. \end{aligned} \quad (45)$$

The comparison shows that our approach is a natural extension of the continuum theory to the atomic scale, and is suitable for multiscale description of lattice dynamics.

### D. Phonon analysis using symmetry modes

We analyze phonon modes in terms of atomic scale symmetry modes for the square lattice with a harmonic potential shown below.<sup>12</sup>

$$\begin{aligned} V_{\text{sq}} = \sum_{\vec{i}} & \frac{1}{2} A_1 e_1(\vec{i})^2 + \frac{1}{2} A_2 e_2(\vec{i})^2 + \frac{1}{2} A_3 e_3(\vec{i})^2 \\ & + \frac{1}{2} B [s_x(\vec{i})^2 + s_y(\vec{i})^2]. \end{aligned} \quad (46)$$

By solving the Lagrangian equations Eq. (31), we find dispersion relations without using displacement variables explicitly,<sup>16</sup>

$$\begin{aligned} M\omega^2 = & B(1 - \cos k_x)(1 - \cos k_y) \\ & + \frac{1}{2} (A_1 + A_2 + A_3)(1 - \cos k_x \cos k_y) \\ & \pm \left[ \frac{1}{4} (A_1 - A_2 + A_3)^2 (\cos k_x - \cos k_y)^2 \right. \\ & \left. + \frac{1}{4} (A_1 + A_2 - A_3)^2 \sin^2 k_x \sin^2 k_y \right]^{1/2}, \end{aligned} \quad (47)$$

which has been also obtained using displacement variables in Ref. 12. Furthermore, from the Lagrangian equations, we find normalized symmetry-mode squared

amplitude for the phonons of the square lattice with a monatomic basis, which represents how square plaquettes of four atoms distort when the lattice vibrates in each phonon mode. Corresponding expressions for general case, as well as for three special cases, are shown in Table I, where  $\beta_1 = 1 - \cos k_x \cos k_y$ ,  $\beta_2 = -\sin k_x \sin k_y$ ,  $\beta_3 = \cos k_x - \cos k_y$ ,  $\beta_4 = (1 - \cos k_x)(1 - \cos k_y)$ ,  $\beta_5 = (1 + \cos k_x)(1 + \cos k_y)$ , and  $a = (A_1 - A_2 + A_3)/(A_1 + A_2 - A_3)$ . These expressions are also plotted within the first Brillouin zone of the square lattice in Figs. 6, 7, 8, 9, and 10 for  $a = 0, 0.1, 1, 10$ , and  $\infty$ , respectively. The modes represented by the twelve panels in each figure are given in the caption for Fig. 6.

We discuss overall features of these results. First, the squared amplitudes for the upper and lower branches show symmetries. The squared amplitude of the  $e_1$  mode in the upper (lower) branch is identical to the squared amplitude of  $r$  mode in the lower (upper) branch (see general expressions in Table I). Similar relations exist between  $e_2$  and  $e_3$ , between  $s_x$  and  $s_y$ , between  $t_x$  and  $t_y$ , between  $s_+$  and  $s_-$ , and between  $t_+$  and  $t_-$ . Second, the squared amplitude is highly anisotropic. For  $a = 0.1 - \infty$ , modes  $e_1$  and  $e_3$  in the upper branch (equivalently,  $r$  and  $e_2$  in the lower branch) are dominant around  $\vec{k} = (\pm\pi, 0)$ ,  $(0, \pm\pi)$ , and around the bond directions from the zone center [panel (a)'s and (c)'s in Figs. 7 - 10]. In contrast, mode  $e_2$  in the upper branch (equivalently, mode  $e_3$  in the lower branch) is dominant mainly

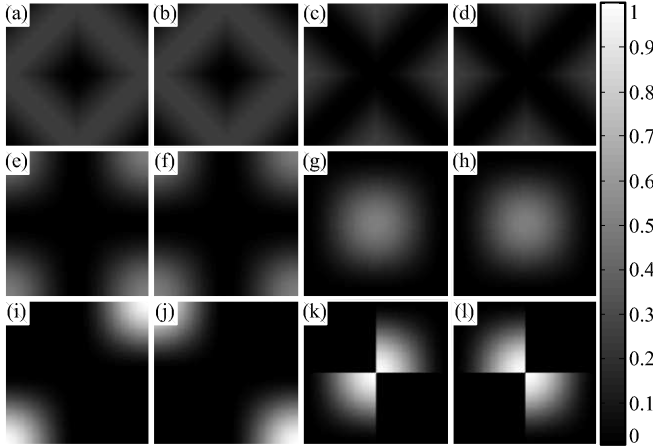


FIG. 6: Normalized symmetry-mode squared amplitude for phonons within the first Brillouin zone of the square lattice for  $a = 0$ , where  $a = (A_1 - A_2 + A_3)/(A_1 + A_2 - A_3)$ . For the upper branch, the twelve panels correspond to (a) $|e_1|^2$ , (b) $|e_2|^2$ , (c) $|e_3|^2$ , (d) $|r|^2$ , (e) $|s_x|^2$ , (f) $|s_y|^2$ , (g) $|t_x|^2$ , (h) $|t_y|^2$ , (i) $|s_+|^2$ , (j) $|s_-|^2$ , (k) $|t_+|^2$ , and (l) $|t_-|^2$ . For the lower branch, they correspond to (a) $|r|^2$ , (b) $|e_3|^2$ , (c) $|e_2|^2$ , (d) $|e_1|^2$ , (e) $|s_y|^2$ , (f) $|s_x|^2$ , (g) $|t_y|^2$ , (h) $|t_x|^2$ , (i) $|s_-|^2$ , (j) $|s_+|^2$ , (k) $|t_-|^2$ , and (l) $|t_+|^2$ .

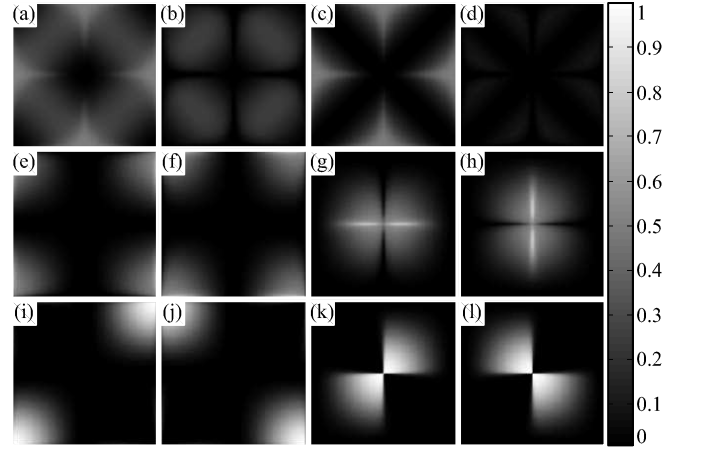


FIG. 7: Normalized symmetry-mode squared amplitude for the phonons for  $a = 0.1$ . Refer to Fig. 6 for the description of each panel.

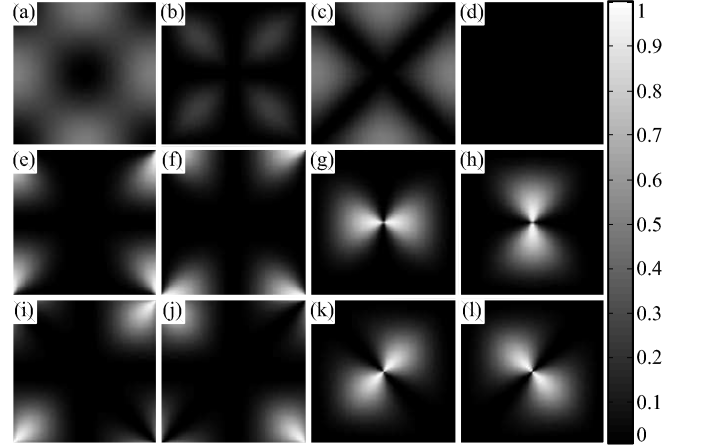


FIG. 8: Normalized symmetry-mode squared amplitude for the phonons for  $a = 1$ . Refer to Fig. 6 for the description of each panel.

in the region around zone-diagonal directions, which becomes narrower as the parameter  $a$  increases [panel (b)'s in Figs. 7 - 10]. Third, the squared amplitude also depends strongly on the magnitude of wavevector  $\vec{k}$ . Near the zone center, where  $k \approx 0$ ,  $t_x$ ,  $t_y$ ,  $t_+$ , and  $t_-$  modes are dominant [panel (g)'s, (h)'s, (k)'s, and (l)'s in Figs. 6 - 10], whereas near the zone corners, where  $\vec{k} \approx (\pm\pi, \pm\pi)$ ,  $s_x$ ,  $s_y$ ,  $s_+$ , and  $s_-$  modes are dominant [panel (e)'s, (f)'s, (i)'s, and (j)'s in Figs. 6 - 10]. Generally, the squared amplitudes for  $s_x$ ,  $s_y$ ,  $s_+$  and  $s_-$  at  $\vec{k}$  are identical to those for  $t_x$ ,  $t_y$ ,  $t_+$ , and  $t_-$  at  $(\pi, \pi) - \vec{k}$ , respectively. Between  $k \approx 0$  and  $k \approx (\pm\pi, \pm\pi)$ ,  $e_1$ ,  $e_2$ ,  $e_3$ , and  $r$  mode amplitudes are prominent [panel (a) - (d)'s in Figs. 6 - 10]. Fourth, the squared amplitudes depend on the moduli,

Mode	General expression	$a = 0$	$a = 1$		$a = \infty$
	upper/lower branch	upper/lower branch	upper branch	lower branch	upper/lower branch
$ e_1 ^2$	$\frac{1}{8} \left( \beta_1 \pm \frac{\beta_2^2 + a\beta_3^2}{\sqrt{\beta_2^2 + a^2\beta_3^2}} \right)$	$\frac{1}{8} (\beta_1 \pm  \beta_2 )$	$\frac{\beta_1}{4}$	0	$\frac{1}{8} (\beta_1 \pm  \beta_3 )$
$ e_2 ^2$	$\frac{1}{8} \left( \beta_1 \pm \frac{\beta_2^2 - a\beta_3^2}{\sqrt{\beta_2^2 + a^2\beta_3^2}} \right)$	$\frac{1}{8} (\beta_1 \pm  \beta_2 )$	$\frac{\beta_2^2}{4\beta_1}$	$\frac{\beta_3^2}{4\beta_1}$	$\frac{1}{8} (\beta_1 \mp  \beta_3 )$
$ e_3 ^2$	$\frac{1}{8} \left( \beta_1 \mp \frac{\beta_2^2 - a\beta_3^2}{\sqrt{\beta_2^2 + a^2\beta_3^2}} \right)$	$\frac{1}{8} (\beta_1 \mp  \beta_2 )$	$\frac{\beta_2^2}{4\beta_1}$	$\frac{\beta_3^2}{4\beta_1}$	$\frac{1}{8} (\beta_1 \pm  \beta_3 )$
$ r ^2$	$\frac{1}{8} \left( \beta_1 \mp \frac{\beta_2^2 + a\beta_3^2}{\sqrt{\beta_2^2 + a^2\beta_3^2}} \right)$	$\frac{1}{8} (\beta_1 \mp  \beta_2 )$	0	$\frac{\beta_1}{4}$	$\frac{1}{8} (\beta_1 \mp  \beta_3 )$
$ s_x ^2$	$\frac{\beta_4}{8} \left( 1 \mp \frac{a\beta_3}{\sqrt{\beta_2^2 + a^2\beta_3^2}} \right)$	$\frac{\beta_4}{8}$	$\frac{\beta_4}{8\beta_1} (\beta_1 - \beta_3)$	$\frac{\beta_4}{8\beta_1} (\beta_1 + \beta_3)$	$\frac{\beta_4}{8} [1 \mp \text{sign}(\beta_3)]$
$ s_y ^2$	$\frac{\beta_4}{8} \left( 1 \pm \frac{a\beta_3}{\sqrt{\beta_2^2 + a^2\beta_3^2}} \right)$	$\frac{\beta_4}{8}$	$\frac{\beta_4}{8\beta_1} (\beta_1 + \beta_3)$	$\frac{\beta_4}{8\beta_1} (\beta_1 - \beta_3)$	$\frac{\beta_4}{8} [1 \pm \text{sign}(\beta_3)]$
$ t_x ^2$	$\frac{\beta_5}{8} \left( 1 \mp \frac{a\beta_3}{\sqrt{\beta_2^2 + a^2\beta_3^2}} \right)$	$\frac{\beta_5}{8}$	$\frac{\beta_5}{8\beta_1} (\beta_1 - \beta_3)$	$\frac{\beta_5}{8\beta_1} (\beta_1 + \beta_3)$	$\frac{\beta_5}{8} [1 \mp \text{sign}(\beta_3)]$
$ t_y ^2$	$\frac{\beta_5}{8} \left( 1 \pm \frac{a\beta_3}{\sqrt{\beta_2^2 + a^2\beta_3^2}} \right)$	$\frac{\beta_5}{8}$	$\frac{\beta_5}{8\beta_1} (\beta_1 + \beta_3)$	$\frac{\beta_5}{8\beta_1} (\beta_1 - \beta_3)$	$\frac{\beta_5}{8} [1 \pm \text{sign}(\beta_3)]$
$ s_+ ^2$	$\frac{\beta_4}{8} \left( 1 \mp \frac{\beta_2}{\sqrt{\beta_2^2 + a^2\beta_3^2}} \right)$	$\frac{\beta_4}{8} [1 \mp \text{sign}(\beta_2)]$	$\frac{\beta_4}{8\beta_1} (\beta_1 - \beta_2)$	$\frac{\beta_4}{8\beta_1} (\beta_1 + \beta_2)$	$\frac{\beta_4}{8}$
$ s_- ^2$	$\frac{\beta_4}{8} \left( 1 \pm \frac{\beta_2}{\sqrt{\beta_2^2 + a^2\beta_3^2}} \right)$	$\frac{\beta_4}{8} [1 \pm \text{sign}(\beta_2)]$	$\frac{\beta_4}{8\beta_1} (\beta_1 + \beta_2)$	$\frac{\beta_4}{8\beta_1} (\beta_1 - \beta_2)$	$\frac{\beta_4}{8}$
$ t_+ ^2$	$\frac{\beta_5}{8} \left( 1 \mp \frac{\beta_2}{\sqrt{\beta_2^2 + a^2\beta_3^2}} \right)$	$\frac{\beta_5}{8} [1 \mp \text{sign}(\beta_2)]$	$\frac{\beta_5}{8\beta_1} (\beta_1 - \beta_2)$	$\frac{\beta_5}{8\beta_1} (\beta_1 + \beta_2)$	$\frac{\beta_5}{8}$
$ t_- ^2$	$\frac{\beta_5}{8} \left( 1 \pm \frac{\beta_2}{\sqrt{\beta_2^2 + a^2\beta_3^2}} \right)$	$\frac{\beta_5}{8} [1 \pm \text{sign}(\beta_2)]$	$\frac{\beta_5}{8\beta_1} (\beta_1 + \beta_2)$	$\frac{\beta_5}{8\beta_1} (\beta_1 - \beta_2)$	$\frac{\beta_5}{8}$

TABLE I: Normalized symmetry-mode squared amplitude for phonons within the first Brillouin zone of the square lattice. For  $\pm$  and  $\mp$ , the upper sign corresponds to the upper branch, and the lower sign the lower branch.  $\beta_1 = 1 - \cos k_x \cos k_y$ ,  $\beta_2 = -\sin k_x \sin k_y$ ,  $\beta_3 = \cos k_x - \cos k_y$ ,  $\beta_4 = (1 - \cos k_x)(1 - \cos k_y)$ ,  $\beta_5 = (1 + \cos k_x)(1 + \cos k_y)$ ,  $a = (A_1 - A_2 + A_3)/(A_1 + A_2 - A_3)$ , and  $\text{sign}(x) = x/|x|$ . The amplitudes are normalized by  $|e_1|^2 + |e_2|^2 + |e_3|^2 + |r|^2 + |s_x|^2 + |s_y|^2 + |t_x|^2 + |t_y|^2 = 1$ .

$A_1$ ,  $A_2$ , and  $A_3$ , through the parameter  $a$ , but are independent of  $B$ . In particular, the general expressions bring additional symmetries for special cases of  $a = 0$ ,  $1$ , and  $\infty$ , which correspond to  $A_1 + A_3 = A_2$ ,  $A_2 = A_3$ , and  $A_1 + A_2 = A_3$ , respectively (Table I). Mode  $r$  in the upper and  $e_1$  in the lower branches vanish completely for  $A_2 = A_3$ , which signifies the symmetry discussed below.

We further comment on two aspects of the results, specific to certain modes or values of  $a$ . First, as mentioned above, if  $a = 1$ , or  $A_2 = A_3$ , the upper phonon branch includes no rotational mode  $r$ , and the lower branch includes no area-changing mode  $e_1$ , which is interpreted in the following way. If the two shape-changing modes,  $e_2$  and  $e_3$ , have identical moduli, the lattice sustains isotropic phonon dispersion in the long wavelength limit, in which the lattice behaves like an isotropic continuous medium. Such medium would support longitudinal phonon modes in the upper branch and transverse phonon modes in the lower branch: the former rotationless and the latter locally area-preserving. For finite wavelengths, the phonon dispersion is not isotropic, and the phonon modes are not longitudinal, nor transverse. However, the upper and lower branches of phonon

modes remain locally rotationless and area-preserving respectively even for finite wavelength, if the two shape-changing modes have identical moduli. Panel (d)'s in Figs. 7, 8, and 9 show that amplitudes for these modes remain relatively small for a wide range of  $a$ . Second, the upper and lower branches of phonon modes at  $\vec{k} = (\pi, 0)$  are longitudinal and transverse, as shown in Figs. 11(a) and 11(b), respectively. Therefore, the phonon at  $\vec{k} = (\pi, 0)$  in the upper branch consists of  $e_1$  and  $e_3$  modes, and that in the lower branch of  $e_2$  and  $r$  modes, which explains the large contribution of these modes near  $\vec{k} = (\pm\pi, 0)$  and  $(0, \pm\pi)$  and around the bond direction from the zone center [panel (a)'s and (c)'s in Figs. 6 - 10]. For  $a = 0$ , or  $A_1 + A_3 = A_2$ , the two phonon modes at  $\vec{k} = (\pi, 0)$  shown in Fig. 11 have the same net modulus and therefore are degenerate, which gives rise to the equal contribution of the four modes,  $e_1$ ,  $e_2$ ,  $e_3$  and  $r$  at this  $\vec{k}$  point, as shown in panels (a) - (d) in Fig. 6.

Understanding how different modes contribute to various parts in the  $k$ -space could be useful, for example, to gain insight in materials with electron-phonon cou-

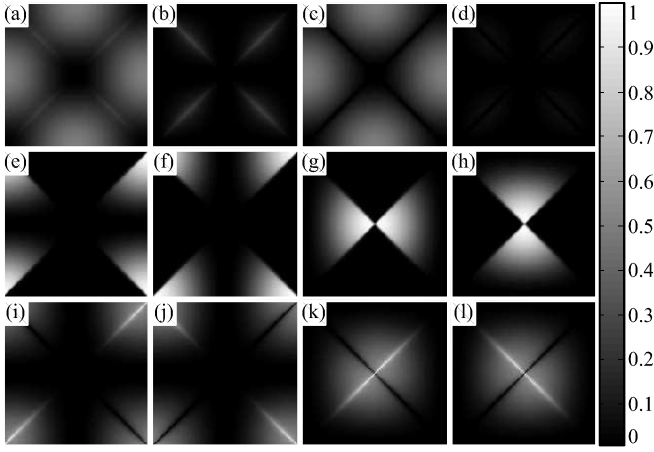


FIG. 9: Normalized symmetry-mode squared amplitude for the phonons for  $a = 10$ . Refer to Fig. 6 for the description of each panel.

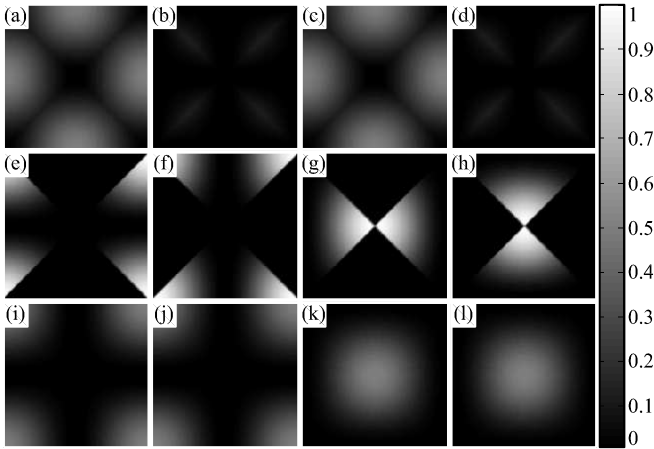


FIG. 10: Normalized symmetry-mode squared amplitude for the phonons for  $a = \infty$ . Refer to Fig. 6 for the description of each panel.

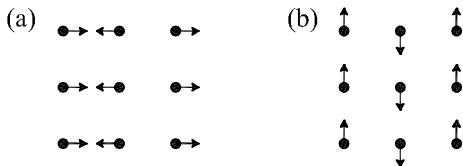


FIG. 11: (a) Upper and (b) lower branch phonon modes at  $\vec{k} = (\pi, 0)$  for the two-dimensional square lattice with a monatomic basis.

pling, such as, manganites, phonon-mediated superconductors, and materials near structural phase transition. The above analysis demonstrates the advantage of the approach based on symmetry mode for atomic scale description of lattice dynamics.

### III. QUANTUM MECHANICAL FORMALISM

#### A. One-dimensional lattice with a monatomic basis

It is necessary to consider quantum mechanical aspects of lattice dynamics for phenomena such as low temperature specific heat, electron-phonon interaction, and polarons. In this section, we extend the symmetry-based atomic scale description of lattice dynamics to the quantum mechanical formalism. Commutation relations between the coordinate operators and their conjugate momentum operators lie at the core of quantum mechanics, which we establish here for the symmetry modes.

First, we consider the one-dimensional chain studied in Section II.A. The conjugate momenta for the two modes,  $P_e(i)$  and  $P_t(i)$  are

$$P_e(i) = \frac{\partial L}{\partial \dot{e}(i)} = \frac{M}{2} \dot{e}(i) = \frac{1}{2\sqrt{2}}(p_{i+1} - p_i), \quad (48)$$

$$P_t(i) = \frac{\partial L}{\partial \dot{t}(i)} = \frac{M}{2} \dot{t}(i) = \frac{1}{2\sqrt{2}}(p_{i+1} + p_i), \quad (49)$$

where  $p_i$  represents the momentum of the atom at site  $i$ . From known commutation relations between momentum and displacement operators  $\hat{p}_i$  and  $\hat{u}_j$ , we find the following commutation relations between the operators for modes and their conjugate momenta with the same site index  $i$ ,

$$[P_a(i), b(i)] = \frac{\hbar}{2i} \delta_{ab},$$

where  $a, b \in \{e, t\}$ . The  $1/2$  factor is related to the number of atoms in each motif. Unlike displacement variables, the commutation relation between a mode at  $i$  and a conjugate momentum at  $i+1$  or  $i-1$  is not zero, since they share an atom, as shown below.

$$[P_t(i), t(i \pm 1)] = [P_e(i), t(i+1)] = [P_t(i), e(i-1)] = \frac{\hbar}{4i},$$

$$[P_e(i), e(i \pm 1)] = [P_t(i), e(i+1)] = [P_e(i), t(i-1)] = \frac{-\hbar}{4i}.$$

The commutation relations between the momentum and the mode, defined at sites further than the nearest neighbors, vanish.

The above relations are also established graphically. For example,  $[P_e(i), t(i+1)]$  is found from the drawing in Fig. 12, where  $P_e(i)$  and  $t(i+1)$  are represented with arrows. We treat the arrows as unit vectors, and find the

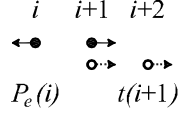


FIG. 12: Graph to find commutation relation,  $[P_e(i), t(i+1)]$ .

sum of scalar products of unit vectors defined at the same sites, which after being multiplied by  $\hbar/(2^2i)$ , lead to the commutation relation. From the graphical rule and the symmetry of the modes, the following commutations are obtained, where  $a, b \in \{e, t\}$ .

$$[P_a(i), b(j)] = [P_b(j), a(i)], \quad (50)$$

$$[P_e(i), t(j)] = -[P_t(i), e(j)]. \quad (51)$$

The commutation relations in reciprocal space are calculated from the relations,

$$[P_a(k), b(k')] = \delta_{k', -k} \sum_j [P_a(i=0), b(j)] e^{ikj}, \quad (52)$$

which are shown in Table II. The results found here are applicable, for example, for the study of quantum mechanical dynamics of non-linear excitations mentioned in Section II.A.

	$\frac{i}{\hbar} P_e(k)$	$\frac{i}{\hbar} P_t(k)$
$e(-k)$	$\frac{1}{2}(1 - \cos k)$	$-\frac{i}{2} \sin k$
$t(-k)$	$\frac{i}{2} \sin k$	$\frac{1}{2}(1 + \cos k)$

TABLE II: Commutation relation,  $[\frac{i}{\hbar} P_a(k), b(-k)]$ , between symmetry modes and their conjugate momenta for the one-dimensional chain in reciprocal space.

### B. Two-dimensional square lattice with a monatomic basis

Quantum mechanical nature of lattice is also important for two or three-dimensional lattices, for example, near the structural phase transitions. In this subsection, we find quantum mechanical commutation relations for the symmetry modes and their conjugate momenta for the square lattice studied in Section II.B.

Conjugate momenta for the atomic scale symmetry

modes are as follows.

$$\begin{aligned} P_{e_1}(\vec{i}) &= \frac{M}{4} \dot{e}_1(\vec{i}) = \frac{1}{8\sqrt{2}} \left( -p_i^x - p_i^y + p_{i+10}^x - p_{i+10}^y \right. \\ &\quad \left. - p_{i+01}^x + p_{i+01}^y + p_{i+11}^x + p_{i+11}^y \right), \\ P_{e_2}(\vec{i}) &= \frac{M}{4} \dot{e}_2(\vec{i}) = \frac{1}{8\sqrt{2}} \left( -p_i^x - p_i^y - p_{i+10}^x + p_{i+10}^y \right. \\ &\quad \left. + p_{i+01}^x - p_{i+01}^y + p_{i+11}^x + p_{i+11}^y \right), \\ P_{e_3}(\vec{i}) &= \frac{M}{4} \dot{e}_3(\vec{i}) = \frac{1}{8\sqrt{2}} \left( -p_i^x + p_i^y + p_{i+10}^x + p_{i+10}^y \right. \\ &\quad \left. - p_{i+01}^x - p_{i+01}^y + p_{i+11}^x - p_{i+11}^y \right), \\ P_r(\vec{i}) &= \frac{M}{4} \dot{r}(\vec{i}) = \frac{1}{8\sqrt{2}} \left( p_i^x - p_i^y + p_{i+10}^x + p_{i+10}^y \right. \\ &\quad \left. - p_{i+01}^x - p_{i+01}^y - p_{i+11}^x + p_{i+11}^y \right), \\ P_{s_x}(\vec{i}) &= \frac{M}{4} \dot{s}_x(\vec{i}) = \frac{1}{8} \left( p_i^x - p_{i+10}^x - p_{i+01}^x + p_{i+11}^x \right), \\ P_{s_y}(\vec{i}) &= \frac{M}{4} \dot{s}_y(\vec{i}) = \frac{1}{8} \left( p_i^y - p_{i+10}^y - p_{i+01}^y + p_{i+11}^y \right), \\ P_{t_x}(\vec{i}) &= \frac{M}{4} \dot{t}_x(\vec{i}) = \frac{1}{8} \left( p_i^x + p_{i+10}^x + p_{i+01}^x + p_{i+11}^x \right), \\ P_{t_y}(\vec{i}) &= \frac{M}{4} \dot{t}_y(\vec{i}) = \frac{1}{8} \left( p_i^y + p_{i+10}^y + p_{i+01}^y + p_{i+11}^y \right). \end{aligned}$$

From the fundamental commutation relations for displacement operators and momentum operators,

$$\begin{aligned} [p_i^x, u_j^x] &= [p_i^y, u_j^y] = \frac{\hbar}{i} \delta_{\vec{i}, \vec{j}}, \\ [p_i^x, u_j^y] &= [p_i^y, u_j^x] = 0, \end{aligned}$$

the commutation relations between modes and their conjugate momenta are calculated in a straight forward way.

However, it is more convenient to use the graphical method, explained for the one-dimensional chain in the previous subsection. The above fundamental commutation relations for  $\vec{i} = \vec{j}$  have the form of

$$\begin{aligned} \hat{x} \cdot \hat{x} &= \hat{y} \cdot \hat{y} = 1, \\ \hat{x} \cdot \hat{y} &= \hat{y} \cdot \hat{x} = 0, \end{aligned}$$

except for the factor  $\hbar/i$ , where  $\hat{x}$  and  $\hat{y}$  represent unit vectors, not operators. Therefore, the commutation relation  $[P_a(\vec{i}), b(\vec{j})]$ , where  $a$  and  $b$  represent the eight atomic scale modes, is found from the drawings of  $a$  and  $b$  modes on the square lattice. The sum of the scalar products of the unit vectors at the sites shared by the two modes, multiplied by  $\hbar/(4^2i)$ , gives the commutation of the two operators. (The multiplication factor after  $\hbar/i$  is associated with the number of atoms in the motif for the lattice with a monatomic basis, that is 4 for the square lattice and 2 for the chain.) For example,  $[P_{e_1}(\vec{i}), e_2(\vec{i} + 11)]$  is found from Fig. 13, as follows

$$[P_{e_1}(\vec{i}), e_2(\vec{i} + 11)] = \frac{\hbar}{4^2i} (-1). \quad (53)$$



	$\frac{i}{\hbar} P_{e1}(\vec{k})$	$\frac{i}{\hbar} P_{e2}(\vec{k})$	$\frac{i}{\hbar} P_{e3}(\vec{k})$	$\frac{i}{\hbar} P_r(\vec{k})$	$\frac{i}{\hbar} P_{sx}(\vec{k})$	$\frac{i}{\hbar} P_{sy}(\vec{k})$	$\frac{i}{\hbar} P_{tx}(\vec{k})$	$\frac{i}{\hbar} P_{ty}(\vec{k})$
$e_1(-\vec{k})$	$\frac{1-C_{kx}C_{ky}}{4}$	$\frac{S_{kx}S_{ky}}{4}$	$\frac{-C_{kx}+C_{ky}}{4}$	0	$\frac{i(1-C_{kx})S_{ky}}{4\sqrt{2}}$	$\frac{i(1-C_{ky})S_{kx}}{4\sqrt{2}}$	$\frac{i(1+C_{ky})S_{kx}}{-4\sqrt{2}}$	$\frac{i(1+C_{kx})S_{ky}}{-4\sqrt{2}}$
$e_2(-\vec{k})$	$\frac{S_{kx}S_{ky}}{4}$	$\frac{1-C_{kx}C_{ky}}{4}$	0	$\frac{-C_{kx}+C_{ky}}{4}$	$\frac{i(1-C_{ky})S_{kx}}{4\sqrt{2}}$	$\frac{i(1-C_{kx})S_{ky}}{4\sqrt{2}}$	$\frac{i(1+C_{kx})S_{ky}}{-4\sqrt{2}}$	$\frac{i(1+C_{ky})S_{kx}}{-4\sqrt{2}}$
$e_3(-\vec{k})$	$\frac{-C_{kx}+C_{ky}}{4}$	0	$\frac{1-C_{kx}C_{ky}}{4}$	$\frac{-S_{kx}S_{ky}}{4}$	$\frac{i(1-C_{kx})S_{ky}}{4\sqrt{2}}$	$\frac{i(1-C_{ky})S_{kx}}{-4\sqrt{2}}$	$\frac{i(1+C_{ky})S_{kx}}{-4\sqrt{2}}$	$\frac{i(1+C_{kx})S_{ky}}{4\sqrt{2}}$
$r(-\vec{k})$	0	$\frac{-C_{kx}+C_{ky}}{4}$	$\frac{-S_{kx}S_{ky}}{4}$	$\frac{1-C_{kx}C_{ky}}{4}$	$\frac{i(1-C_{ky})S_{kx}}{-4\sqrt{2}}$	$\frac{i(1-C_{kx})S_{ky}}{4\sqrt{2}}$	$\frac{i(1+C_{kx})S_{ky}}{4\sqrt{2}}$	$\frac{i(1+C_{ky})S_{kx}}{-4\sqrt{2}}$
$s_x(-\vec{k})$	$\frac{i(1-C_{kx})S_{ky}}{-4\sqrt{2}}$	$\frac{i(1-C_{ky})S_{kx}}{-4\sqrt{2}}$	$\frac{i(1-C_{kx})S_{ky}}{-4\sqrt{2}}$	$\frac{i(1-C_{ky})S_{kx}}{4\sqrt{2}}$	$\frac{(1-C_{kx})(1-C_{ky})}{4}$	0	$\frac{-S_{kx}S_{ky}}{4}$	0
$s_y(-\vec{k})$	$\frac{i(1-C_{ky})S_{kx}}{-4\sqrt{2}}$	$\frac{i(1-C_{kx})S_{ky}}{-4\sqrt{2}}$	$\frac{i(1-C_{ky})S_{kx}}{4\sqrt{2}}$	$\frac{i(1-C_{kx})S_{ky}}{-4\sqrt{2}}$	0	$\frac{(1-C_{kx})(1-C_{ky})}{4}$	0	$\frac{-S_{kx}S_{ky}}{4}$
$t_x(-\vec{k})$	$\frac{i(1+C_{ky})S_{kx}}{4\sqrt{2}}$	$\frac{i(1+C_{kx})S_{ky}}{4\sqrt{2}}$	$\frac{i(1+C_{ky})S_{kx}}{4\sqrt{2}}$	$\frac{i(1+C_{kx})S_{ky}}{-4\sqrt{2}}$	$\frac{-S_{kx}S_{ky}}{4}$	0	$\frac{(1+C_{kx})(1+C_{ky})}{4}$	0
$t_y(-\vec{k})$	$\frac{i(1+C_{kx})S_{ky}}{4\sqrt{2}}$	$\frac{i(1+C_{ky})S_{kx}}{4\sqrt{2}}$	$\frac{i(1+C_{kx})S_{ky}}{-4\sqrt{2}}$	$\frac{i(1+C_{ky})S_{kx}}{4\sqrt{2}}$	0	$\frac{-S_{kx}S_{ky}}{4}$	0	$\frac{(1+C_{kx})(1+C_{ky})}{4}$

TABLE III: Commutation relation,  $[\frac{i}{\hbar} P_a(\vec{k}), b(-\vec{k})]$ , between symmetry modes and their conjugate momenta for the two-dimensional square lattice in reciprocal space.  $C_{kx}$ ,  $C_{ky}$ ,  $S_{kx}$ , and  $S_{ky}$  represent  $\cos k_x$ ,  $\cos k_y$ ,  $\sin k_x$ , and  $\sin k_y$ , respectively.

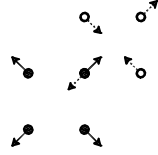


FIG. 13: Graph to find commutation relation,  $[P_{e1}(\vec{i}), e_2(\vec{i} + 11)]$ .

Presented graphical method is also useful to find the following symmetry-related properties of the commutation relations, where  $a$  and  $b$  represent any of the eight modes, and *even* and *odd* represent the modes with even symmetry under point reflection, namely,  $e_1$ ,  $e_2$ ,  $e_3$ ,  $r$ , and the modes with odd symmetry, namely,  $s_x$ ,  $s_y$ ,  $t_x$ ,  $t_y$ , respectively.

$$\begin{aligned}
[P_a(\vec{i}), b(\vec{i})] &= \frac{1}{4} \frac{\hbar}{i} \delta_{ab}, \\
[P_a(\vec{i}), b(\vec{j})] &= [P_b(\vec{j}), a(\vec{i})], \\
[P_{even}(\vec{i}), even'(\vec{j})] &= [P_{even'}(\vec{i}), even(\vec{j})], \\
[P_{even}(\vec{i}), odd(\vec{j})] &= -[P_{odd}(\vec{i}), even(\vec{j})], \\
[P_{odd}(\vec{i}), odd'(\vec{j})] &= [P_{odd'}(\vec{i}), odd(\vec{j})].
\end{aligned}$$

The commutation relations in reciprocal space are found

from the relation

$$[P_a(\vec{k}), b(\vec{k}')] = \delta_{\vec{k}', -\vec{k}} \sum_{\vec{j}} [P_a(\vec{i} = 0), b(\vec{j})] e^{i\vec{k} \cdot \vec{j}}, \quad (54)$$

which are provided in Table III.

#### IV. SUMMARY

In this article, we have presented mode-based atomic scale description of lattice dynamics. It is found that not only the potential energy but also the kinetic energy is described in terms of the atomic scale modes, for which the inclusion of the rigid modes is essential. This approach has been demonstrated for the one-dimensional chain and the two-dimensional square lattice with a monatomic basis. The comparison with a continuum model has shown that our approach is suitable for multiscale description of lattice dynamics. Phonon analysis in terms of symmetry modes have revealed the momentum dependence associated with underlying symmetry of the modes. The approach has been extended to quantum mechanics, and the commutation relations have been obtained. We expect that this method would be useful in describing atomic scale lattice dynamics in systems with strong anharmonicity and complex energy landscape, which can be compared with the results from time-resolved x-ray experiments.

\* Electronic address: kenahn@njit.edu

<sup>1</sup> M. Rini, R. Tobey, N. Dean, J. Itatani, Y. Tomioka, Y. Tokura, R. W. Schoenlein, and A. Cavalleri, Nature (London) 449, 72 (2007).

<sup>2</sup> M. B. Salamon and M. Jaime, Rev. Mod. Phys. **73**, 583 (2001).

- <sup>3</sup> A. J. Millis, Nature (London) **392**, 147 (1998).
- <sup>4</sup> S. Jin, T. H. Tiefel, M. McCormack, R. A. Fastnacht, R. Ramesh, and L. H. Chen, Science **264**, 413 (1994).
- <sup>5</sup> J. M. Tranquada, B. J. Sternlieb, J. D. Axe, Y. Nakamura, and S. Uchida, Nature (London) **375**, 561 (1995).
- <sup>6</sup> S. A. Kivelson, I. P. Bindloss, E. Fradkin, V. Oganesyan, J. M. Tranquada, A. Kapitulnik, and C. Howald, Rev. Mod. Phys. **75**, 1201 (2003).
- <sup>7</sup> V. Kiryukhin, New J. Phys. **6** 155 (2004).
- <sup>8</sup> K. H. Ahn, T. Lookman and A. R. Bishop, Nature (London) **428**, 401 (2004).
- <sup>9</sup> See, e.g., K. J. Gaffney and H. N. Chapman, Science **316**, 1444 (2005), and references therein.
- <sup>10</sup> S.R. Shenoy, T. Lookman, A. Saxena, and A. R. Bishop, Phys. Rev. B **60**, R12 537 (1999).
- <sup>11</sup> T. Lookman, S. R. Shenoy, K. Ø. Rasmussen, A. Saxena, and A. R. Bishop, Phys. Rev. B **67**, 024114 (2003).
- <sup>12</sup> K. H. Ahn, T. Lookman, A. Saxena, and A. R. Bishop, Phys. Rev. B **68**, 092101 (2003).
- <sup>13</sup> K. H. Ahn, T. Lookman, A. Saxena and A. R. Bishop, Phys. Rev. B **71**, 212102 (2005).
- <sup>14</sup> J.-X. Zhu, K. H. Ahn, Z. Nussinov, T. Lookman, A. V. Balatsky and A. R. Bishop, Phys. Rev. Lett. **91**, 057004 (2003).
- <sup>15</sup> H. Doh, Y. B. Kim, and K. H. Ahn, Phys. Rev. Lett. **98**, 126407 (2007).
- <sup>16</sup> J. Moon, *Mode-based atomic scale Approach: Classical and Quantum Mechanical Approach* (Senior Thesis, Konkuk University, Seoul, 2006).
- <sup>17</sup> C. Kittel, *Introduction to Solid State Physics*, 8th ed. (John Wiley and Sons, Inc., Singapore, 1986).
- <sup>18</sup> D. Chen, S. Aubry, and G. P. Tsironis, Phys. Rev. Lett. **77**, 4776 (1996).
- <sup>19</sup> Y. A. Kosevich, L. I. Manevitch, and A. V. Savin, Phys. Rev. E **77**, 046603 (2008).
- <sup>20</sup> We note that inverting the relation between  $(s_x(\vec{k}), s_y(\vec{k}))$  and  $(u_k^x, u_k^y)$  is not possible for certain wave vectors, for example, wave vectors with  $k_x=0$  or  $k_y=0$ . In those cases, new constraint equations should be found from the definition of the modes.